

Article

Functional Study of Different Lignocellulases from *Trichoderma guizhouense* NJAU4742 in the Synergistic Degradation of Natural Straw

Tuo Li ^{1,2}, Ronghua Pei ^{1,2}, Jianguo Wang ^{1,2}, Yihao Zhou ^{1,2} and Dongyang Liu ^{1,2,*} 

¹ Key Lab of Organic-Based Fertilizers of China and Jiangsu Provincial Key Lab of Solid Organic Waste Utilization, Nanjing 210095, China; lituo@njau.edu.cn (T.L.); 2021103111@stu.njau.edu.cn (R.P.); 2021103116@stu.njau.edu.cn (J.W.); hao13207067830@163.com (Y.Z.)

² College of Resources and Environmental Sciences, Nanjing Agricultural University, Nanjing 210095, China

* Correspondence: liudongyang@njau.edu.cn; Tel./Fax: +86-25-84396853

Abstract: The enzyme-based degradation of lignocellulose for bioenergy production is an eco-friendly and sustainable approach. This study aimed to elucidate the enzymatic characteristics of endoglucanase (EGL), β -glucosidase (BGL), and xylanase (XYN) from *Trichoderma guizhouense* NJAU4742, and to explore the potential mechanisms underlying their synergistic degradation of different natural substrates. The results demonstrated that the three enzymes possessed remarkable high-temperature catalytic activity, broad pH adaptability, and responsiveness to different metal ions. The functional group absorption peaks of different substrates were shifted and altered after the synergistic action, particularly for C=O and O-H. Simultaneously, the crystallinity index of wheat straw, soybean straw, rice straw, and corn straw decreased by 7.40%, 2.37%, 20.60%, and 7.67%, respectively, compared to CK (natural straw). Additionally, the dense structure of different substrates was destroyed, and the inner parenchyma began to be exposed after the synergistic action, as observed by SEM. These findings offer valuable theoretical guidance for the development of lignocellulase applications.

Keywords: crop straw; lignocellulase; thermal stability; pH sensitivity; metal ion response; synergistic degradation



Citation: Li, T.; Pei, R.; Wang, J.; Zhou, Y.; Liu, D. Functional Study of Different Lignocellulases from *Trichoderma guizhouense* NJAU4742 in the Synergistic Degradation of Natural Straw. *Fermentation* **2024**, *10*, 230. <https://doi.org/10.3390/fermentation10050230>

Academic Editor: Bijoy Biswas

Received: 29 March 2024

Revised: 17 April 2024

Accepted: 22 April 2024

Published: 26 April 2024



Copyright: © 2024 by the authors. Licensee MDPI, Basel, Switzerland. This article is an open access article distributed under the terms and conditions of the Creative Commons Attribution (CC BY) license (<https://creativecommons.org/licenses/by/4.0/>).

1. Introduction

With the increasing population, the demand for fossil fuels has gradually increased [1]. However, the exploitation rate of fossil energy is far less than the consumption rate [2]. In addition, the use of fossil fuels will also increase the emissions of greenhouse gases, exerting an irreversible impact on the sustainable and green development of the environment [3]. In this context, the government agencies and researchers of most countries have begun to focus on green and efficient renewable energy sources. Lignocellulose is the most abundant renewable biological resource and is ubiquitous in the majority of the regions of our planet [4]. Because of characteristics including its wide distribution, renewability, and low cost, lignocellulose is considered a good source of sustainable energy and has been extensively applied in the production of combustible liquid fuels such as ethanol, acetone, and butanol [5,6].

Lignocellulose has a complex structure, with hemicellulose (25–30%) enveloping the cellulose (40–50%) core and lignin (15–20%) forming a more rigid structure around the hemicellulose, making it difficult to biodegrade [7]. This has been a major obstacle to the widespread use of lignocellulose as a green bioenergy source. In recent years, many scientists have explored a range of biological degradation methods for lignocellulose through the study of microorganisms, enzymes, and bioreactors, among other techniques. Microorganisms have high adaptability and diversity, which allows them to adapt to different ecological

environments and types of lignocellulose [8]. However, microbial growth requires a certain temperature, humidity, oxygen, and nutrients. The conditions for degradation are relatively harsh, and odors and harmful gases may be generated during the degradation process, which requires effective treatment and control [9]. Enzyme preparation is another efficient method for degrading lignocellulose. Different types of enzyme preparations can selectively degrade different components of lignocellulose, thereby improving degradation efficiency and product purity [10]. Moreover, the waste produced from the degradation of lignocellulose by enzyme preparations is easier to handle and recycle, making it more environmentally friendly compared to traditional physical and chemical methods [11]. What is more important, enzyme preparations can rapidly complete the reaction with a high reaction rate, which allows for the efficient degradation of lignocellulose and an increased utilization rate of biomass [12]. However, the degradation efficiency of enzyme preparations is easily affected by the physical and chemical structure of lignocellulose, and different types of lignocellulose may require different enzyme preparations for degradation [13]. In addition, some enzyme preparations are susceptible to environmental factors such as temperature and pH, which can lead to a decrease in reaction efficiency [14]. Therefore, it is urgent to develop enzyme preparations with a strong degradation function and relatively high stability, and to study their synergistic effect on the degradation of lignocellulose. This will provide a good theoretical basis for the large-scale application of enzyme preparations.

Due to the complexity of the composition and structure of lignocellulose, microorganisms typically secrete multiple enzyme systems to achieve the synergistic degradation of cellulose during the straw decomposition process [15,16]. Cellulase mainly includes endoglucanase, exoglucanase, and β -glucosidase, responsible for cellulose degradation. Endoglucanase hydrolyzes the β -1,4-glycosidic bonds of amorphous cellulose chains randomly, releasing reducing and non-reducing ends, thereby shortening the cellulose molecules, which are the sites attacked by exoglucanase [17]. Exoglucanase, also known as cellobiohydrolase, cleaves β -1,4-glycosidic bonds from the reducing or non-reducing ends of cellulose chains, producing cellobiose [11]. Although β -glucosidase cannot directly act on long cellulose chains, it can hydrolyze cellobiose into glucose, effectively reducing the inhibitory effect of cellobiose on endo- and exoglucanases [18]. Hemicellulose structures are more complex than those of cellulose, mainly present on the surface of cellulose and wrapped between cellulose microfibrils. Endoxylanase primarily breaks the β -1,4-glycosidic bonds of xylan backbones, reducing the polymerization degree of xylan, while β -xylosidase releases β -xylose by acting on the non-reducing ends of oligosaccharides [19].

As the most common saprotrophic fungus in soil, *Trichoderma* has been extensively studied and applied in the degradation of lignocellulose [20,21]. It has a rich arsenal of lignocellulolytic enzymes that can efficiently break down different components of lignocellulose [22,23]. By optimizing the production and activity of *Trichoderma* enzymes, lignocellulosic resources can be utilized more effectively, promoting the development of biomass conversion. *Trichoderma guizhouense* NJAU4742, an efficient lignocellulose-degrading fungus, was extensively employed for the large-scale production of biofertilizers via co-solid-state fermentation with agricultural crop residues in China [24]. In this study, endoglucanase, β -glucosidase, and xylanase from *Trichoderma guizhouense* NJAU4742 were heterologously expressed, and the characteristics and synergistic effects of these enzymes were thoroughly analyzed. Additionally, four different crop straws were selected as substrates to compare the degradation efficiency of these enzyme preparations. These findings will provide adequate guidance for improving the application of bioenzyme preparations in production.

2. Materials and Methods

2.1. Description of the Experimental Materials in This Study

In this study, the culture media used for strain cultivation, various substrates used for lignocellulosic enzyme activity detection, and different kit information were first sorted out, and their specific information is shown in Table 1.

Table 1. The purity, supplier, and use information of experimental materials related to this study.

Material	Product Information and Suppliers	Purpose
PDA medium	P8931, Solarbio, Shanghai, China	Strain cultivation
Tris-HCl-NaCl buffer (pH 8.0)	prepared in the lab	Protein dialysis
TEV protease	P8112S, NEB, Ipswich, MA, USA	Protein purification
CMC-Na (99%)	9004, Sigma, St. Louis, MO, USA	Enzyme activity assay
p-NPG (98%)	N1252, Sigma, USA	Enzyme activity assay
xylan	X8070-5, Sigma, USA	Enzyme activity assay
RNeasy® Plant Mini Kit	74904, Qiagen, Hilden, Germany	RNA extraction
PrimeScript RT Reagent Kit	RR036A, Takara, Dalian, China	cDNA synthesis

2.2. Cloning and Expression of EGL, BGL, and XYN

The genes encoding endoglucanase (OPB43431.1), β -glucosidase (OPB36250.1), and xylanase (OPB40690.1) involved in this study all originated from *Trichoderma guizhouense* NJAU4742. Firstly, fresh spore suspension of *Trichoderma guizhouense* NJAU4742 was inoculated onto PDA medium and cultured for three days. The mycelia were collected, and total RNA extraction was performed using the RNeasy® Plant Mini Kit (Qiagen, Germany), and cDNA synthesis was completed using the PrimeScript RT Reagent Kit (RR036A, Takara, Dalian, China) according to the manufacturer's instructions. All the CDSs were amplified by PCR using the cDNA as the template, and subsequently introduced into the pPICZ α A vector (Invitrogen, San Diego, CA, USA). *Pichia pastoris* X33 was employed as the expression host, and the correctly connected expression vectors were linearized and introduced [25]. Recombinant transformants were cultured at 30 °C and 170 rpm in a constant-temperature shaker (ZQZY-AF8, Shanghai Zhichu Instrument Co., Ltd., Shanghai, China) for one week, with periodic addition of methanol to induce protein secretion every 24 h. After completion of the cultivation, the fermentation broth was centrifuged at 10,000 \times g rpm for 10 min using the large-capacity centrifuge (Beckman Coulter, Brea, CA, USA), and the supernatant was collected to obtain crude enzyme containing the corresponding protein. Based on the different functions, the different proteins were named EGL, BGL, and XYN, respectively.

2.3. Purification of EGL, BGL, and XYN

The initial enzymes of EGL, BGL, and XYN were concentrated through the ammonium sulfate precipitation method and the resulting precipitates were reconstituted in a pre-cooled solution of 20 mM Tris-HCl and 100 mM NaCl (pH 8.0). Following this, the crude enzymes were dialyzed using a buffer containing 20 mM Tris-HCl and 300 mM NaCl (pH 8.0). The thickened proteins were purified using an NGC Quest 10 Plus instrument (Bio-Rad, Hercules, CA, USA) with a HisSep Ni-NTA 6FF Chromatography Column (Yeasen, Shanghai, China). The proteins that were initially purified underwent further purification as follows: TEV protease (P8112S, NEB, Ipswich, MA, USA) was added to the initially purified protein in a 5 μ L quantity at 4 °C for 20 h, and the resulting mixture was washed using the HisSep Ni-NTA 6FF Chromatography Column (Yeasen, China). The effluent fractions were considered purified proteins without the 6 \times His tag and were further concentrated using a molecular-weight-truncated concentrator (Sartorius 3 kDa, Thermo Fisher, Norristown, PA, USA). The purity of all proteins was evaluated by measuring A280 and using SDS-PAGE.

2.4. Enzymatic Property Evaluation

To assess the lignocellulase activity, the expressed and characterized crude enzymes of EGL, BGL, and XYN were utilized. Endoglucanase (EGL) activity was measured using CMC-Na (Sigma, USA) as the substrate, while β -glucosidase (BGL) activity was assessed using p-NPG (Sigma, USA) in 0.1 M acetate buffer at 50 °C for 30 min, following the method of Liu et al. [26]. Xylanase (XYN) activity was determined by employing oat spelt xylan (Sigma, USA) as the substrate [27]. One unit of enzymatic activity was defined as the quantity of enzymes required to release one μ mol of glucose or pNP per minute

under the assay conditions. The optimal reaction temperature for EGL, BGL, and XYN was determined by evaluating enzyme activity at temperatures ranging from 20 to 100 °C. The enzyme activities were separately determined under different pH gradients, which were set using various buffer solutions at 50 °C, to characterize their pH sensitivity. In addition, different types of metal ions (mainly Fe³⁺, Zn²⁺, Co²⁺, Mn²⁺, Ca²⁺, Mg²⁺, K⁺, Ni²⁺, and Cu²⁺) were added to the enzyme activity assay system with Na₂HPO₄-citrate buffer to evaluate the effects of these metal ions on the enzyme activities. In short, a mixture of pH 4.0 Na₂HPO₄-citric acid buffer, 1% CMC-Na solution, 0.1 M EGL, and 50 µL of 100 mM different metal ion solutions was evenly mixed and incubated in a water bath at 50 °C for 10 min. After cooling, the OD 600 values were measured using a SpectraMax[®] i3x microplate reader (Molecular Devices, Sunnyvale, CA, USA) following the addition of DNS and boiling for 10 min. Additionally, a mixture of 10 mM p-NPG solution, pH 5.0 Na₂HPO₄-citric acid buffer, 100 mM different metal ion solutions, and 5 µL of 0.1 M BGL was incubated in a water bath at 50 °C for 10 min. The reaction was terminated by the addition of 1 M Na₂CO₃ after incubation, and the OD 410 values were measured using a SpectraMax[®] i3x microplate reader (Molecular Devices, Sunnyvale, CA, USA) after cooling. Furthermore, a mixture of pH 7.0 Na₂HPO₄-KH₂PO₄ buffer, 10 mg of xylan, 100 mM different metal ion solutions, and 0.1 M XYN was incubated in a water bath at 65 °C for 10 min. Following the addition of DNS and boiling for 10 min, the OD 600 values were measured using a SpectraMax[®] i3x microplate reader (Molecular Devices, Sunnyvale, CA, USA) after cooling. In all treatments, an equivalent volume of buffer solution was used instead of protein solution as a blank control, and each treatment was repeated three times.

2.5. Enzyme Kinetics Analysis

The enzymatic reaction kinetics equation can reflect the catalytic efficiency of the enzyme [28]. In this study, enzyme kinetics analysis was conducted by measuring the corresponding enzyme activities by setting different substrate concentrations. For EGL, concentrations of 0.2 mg·mL⁻¹, 0.4 mg·mL⁻¹, 0.6 mg·mL⁻¹, 0.8 mg·mL⁻¹, and 1.0 mg·mL⁻¹ CMC-Na were used, which were mixed with Na₂HPO₄-citric acid buffer (pH 4.0) and 0.1 M EGL. After incubating at 50 °C in a water bath for 10 min, enzyme activity was determined using the DNS method. For BGL, concentrations of 0.2 M, 0.4 M, 0.6 M, 0.8 M, 1.0 M, and 1.2 M p-NPG solutions were used as reaction substrates and mixed with Na₂HPO₄-citric acid buffer (pH 5.0) and 0.1 M BGL. After incubating at 50 °C in a water bath for 10 min, the reaction was terminated with Na₂CO₃, and enzyme activity was determined by measuring the OD 410 value using a SpectraMax[®] i3x microplate reader (Molecular Devices, Sunnyvale, CA, USA). For XYN, suspensions of 0.2 mg·mL⁻¹, 0.4 mg·mL⁻¹, 0.6 mg·mL⁻¹, 0.8 mg·mL⁻¹, 1.0 mg·mL⁻¹, and 1.2 mg·mL⁻¹ of xylan were prepared and mixed with Na₂HPO₄-KH₂PO₄ buffer (pH 7.0) and 0.1 M XYN. After incubating at 65 °C for 10 min in a constant-temperature mixer, enzyme activity was determined using the DNS method. After completing the enzymatic reactions, the reaction rates of each enzyme were calculated, and non-linear regression analysis was used to construct the enzymatic reaction kinetics equations.

2.6. Investigation of Synergistic Effects between Different Enzymes

Three different combinations were used to investigate the synergistic effects of different enzymes, including EGL–BGL, EGL–XYN, and EGL–BGL–XYN, respectively. Each enzyme was added at different proportions, and four types of natural crop straws (wheat straw, soybean straw, rice straw, and corn straw) were used as substrates for enzymatic hydrolysis. Specifically, different straw samples were first pulverized using a grinder and passed through a 100-mesh sieve. Then, 980 µL of Na₂HPO₄-citric acid buffer (pH 5.0) was added to 10 mg of straw powder, followed by the addition of 10 µL of 0.05 M EGL and 10 µL of varying concentrations of BGL (ranging from 0.01 M to 0.08 M). The mixture was reacted at 50 °C for 6 h and then centrifuged at 12,000 rpm for 5 min. Subsequently, 500 µL of the supernatant was collected, and the reducing sugar content was determined using the DNS

method [29,30]. The synergy test between EGL and XYN followed a similar procedure, with XYL concentration set at 0.1 M and EGL concentration ranging from 0.01 M to 0.08 M. For the synergy test involving all three enzymes, XYL concentration was set at 0.1 M, while EGL and BGL concentrations varied from 0.01 M to 0.09 M, with five gradients set up. The volume of mixed enzyme solution added to all treatments was 10 μ L. A control group without enzyme addition was included in all treatments, with at least three biological replicates set up for each condition.

Fourier transform infrared spectroscopy (FTIR), X-ray diffraction (XRD), and scanning electron microscopy (SEM) were performed to further analyze the degree of substrate degradation. First, 20 mg of different natural straw substrates were added to centrifuge tubes, followed by the addition of 970 μ L of Na₂HPO₄-citric acid buffer (pH 5.0). Subsequently, 10 μ L of enzyme solution containing 0.1 M EGL, BGL, and XYN, respectively, was added to each tube and mixed well. The reaction was carried out at 50 °C for 6 h. In parallel, inactive enzyme solution was added as a negative control. After the reaction, the straw substrates from different treatments were collected. FTIR detection was performed according to Kim, S.B. et al. [31]. In short, after the enzymatic reaction was completed, the degradation products were collected by centrifugation and air-dried. The dried products were then ground using a ball mill (Retsch MM400, Germany). Subsequently, the powder was sieved through a 100-mesh sieve, mixed with KBr in a ratio of 1:99, and the mixture was crushed into transparent films. FTIR was performed in the infrared mode using a spectrometer (Thermo Nicolet Nexus™ 670) with a wavelength range of 500–4500 cm⁻¹, a scanning interval of 2 mm, and a scan quantity of 128. A KBr resolution of 4 cm⁻¹ was used as a blank to collect background values, and the data were analyzed and processed using OMNIC software (Thermo Scientific, Norristown, PA, USA). XRD analysis was conducted using the X-ray diffractometer (TD-3500, China) in reflection mode with a range of 5–35° and steps of 0.05°. Data analysis was performed using Origin software (Version 9.0, Origin-Lab, Northampton, MA, USA). The crystallinity index (CI) of avicel was calculated using the following formula: CI (%) = (I₀₀₂ - I_{am})/I₀₀₂ * 100. Here, I₀₀₂ represents the scattering intensity of the crystalline area of the sample, and I_{am} represents the scattering intensity of the amorphous area of the sample [32]. For scanning electron microscopy analysis, the samples of degraded straw from different treatments were immediately dehydrated in 5 mL of ice-cold, 200-proof ethanol (Sigma-Aldrich, St. Louis, MO, USA) after fixation with 2.5% glutaraldehyde for two days, point-dried in a critical point dryer (HCP-2, Hitachi High-Technologies Corporation, Tokyo, Japan), and then coated with 60% Au/Pd in a sputter coater (Sputter Coater Baltec SCD500, Bal-Tel) [33]. The surface morphologies of different samples were observed using an S-4800 II field emission scanning electron microscope (Hitachi, Japan).

2.7. Statistical Analysis

All experiments were repeated three times, and the data are presented as mean \pm standard deviation. Statistical analyses were performed using IBM SPSS Statistics software (version 25.0) and visualized with Origin 2021 software. One-way analysis of variance (ANOVA) and Duncan's multiple range test ($p < 0.05$) were used to analyze the data.

3. Results and Discussion

3.1. Enzymatic Property Evaluation of EGL, BGL, and XYN

This study presented phylogenetic trees for EGL, BGL, and XYN through multiple sequence alignments using MEGAX software (Figures S1–S3). The trees revealed that these proteins clustered with most of the selected enzymes and possessed unique enzymatic profiles. Additionally, SDS-PAGE analysis confirmed the successful expression and electrophoretic purity of these proteins, with molecular sizes of approximately 55 kDa, 80 kDa, and 48 kDa, respectively (Figure 1). The enzymatic properties of various enzymes were evaluated under different temperatures, pHs, and metal ion conditions. As shown in Figure 2, the effects of temperature on EGL, BGL, and XYN were examined under various

temperature conditions. The results indicated that EGL had an optimal reaction temperature of 50 °C but showed significant enzyme activity across a wide range of 20–100 °C, highlighting its remarkable adaptability to both low and high temperatures (Figure 2a). Similarly, BGL displayed a peak activity at 50 °C but maintained consistent enzyme activity levels at temperatures between 40–80 °C, with 85% relative activity retained at 30 °C and 40% at 100 °C. These results suggested that BGL shared a similar ability to adapt to a wide range of temperatures, much like EGL (Figure 2b). XYN demonstrated optimal hydrolysis at 65 °C but also exhibited considerable enzyme activity at temperatures ranging from 50–70 °C (Figure 2c). Similar to previous studies, the heterologously expressed endoglucanase (Rum-EGL), β -glucosidase (Fib-BLG), and xylanase (Geo-XYL) from the genera *Ruminiclostridium*, *Fibrobacter*, and *Geofilum*, respectively, exhibited maximal enzymatic activity at 50 °C [25]. However, unlike Fib-BLG and Geo-XYL, which showed more stable enzymatic activity under different pH conditions, the β -glucosidase and xylanase from *Trichoderma guizhouense* NJAU4742 displayed considerable variations in enzymatic activity at different pH levels. In addition, the enzymatic responses of EGL, BGL, and XYN to different pH conditions were evaluated. EGL displayed maximum activity at pH 3.0, with its enzymatic activity almost disappearing at pH 2.0 and decreasing rapidly beyond pH 5.0 (Figure 2d). BGL exhibited optimum activity within the pH range of 4.0–6.0 and displayed a sharp reduction in relative enzyme activity at pH values below 4.0 or above 7.0, indicating its acid-resistant nature (Figure 2e). XYN showed the highest activity at pH 7.0, with relatively high enzyme activity observed at pH 5.0–9.0. Moreover, the impact of different buffer solutions on its relative enzyme activity was significant, especially in the $\text{Na}_2\text{HPO}_4\text{-KH}_2\text{PO}_4$ buffer solution at pH 7.0, where enzyme activity was markedly enhanced compared to other pH buffer solutions (Figure 2f). Moreover, metal ions have been introduced into cell pretreatment and enzymatic hydrolysis processes, with many studies attempting to understand the impact of metal ions on the enzymatic activity of lignocellulose [34,35]. In this investigation, the effect of metal ions on the activity of three different cellulases was examined. The results demonstrated that Co^{2+} displayed a remarkable enhancing effect on the activity of EGL, exhibiting an increase of up to 113.30% compared to the relative enzyme activity without metal ions (Figure 2g). This was speculated to be due to Co^{2+} ions forming salt bridges or coordinate bonds with specific residues in the enzyme protein, thereby promoting the stability of the structure of EGL and conformational changes, which in turn enhanced the catalytic activity of EGL [36]. Conversely, the addition of Fe^{3+} and K^+ resulted in inhibitory effects, leading to a decrease in the relative enzyme activity by 23.45% and 24.46%, respectively, when compared to CK (Figure 2h). Regarding BGL, no significant enhancement was observed with the addition of metal ions. Nevertheless, Fe^{3+} and Cu^{2+} were found to significantly inhibit BGL activity, with the enzyme activity almost disappearing after the addition of Fe^{3+} and the relative enzyme activity dropping to 20.59% of the activity without metal ions after the addition of Cu^{2+} (Figure 2i). The addition of most metal ions led to a significant reduction in XYN activity, particularly Mn^{2+} , Fe^{3+} , Cu^{2+} , and Zn^{2+} . Consistent with previous studies, many cations may interact with the negatively charged parts of proteins, such as carboxyl groups and phosphate groups, thereby affecting the structure and stability of proteins, resulting in the inhibition of enzyme activity. In addition, some metal ions may form unstable enzyme–metal complexes by coordinating with the active sites of enzymes, thereby hindering the catalytic activity of enzymes [37]. However, Mg^{2+} showed a strong promoting effect on XYN, increasing the relative enzyme activity by 35.86% compared to CK, suggesting its potential application in the field of lignocellulose biodegradation.

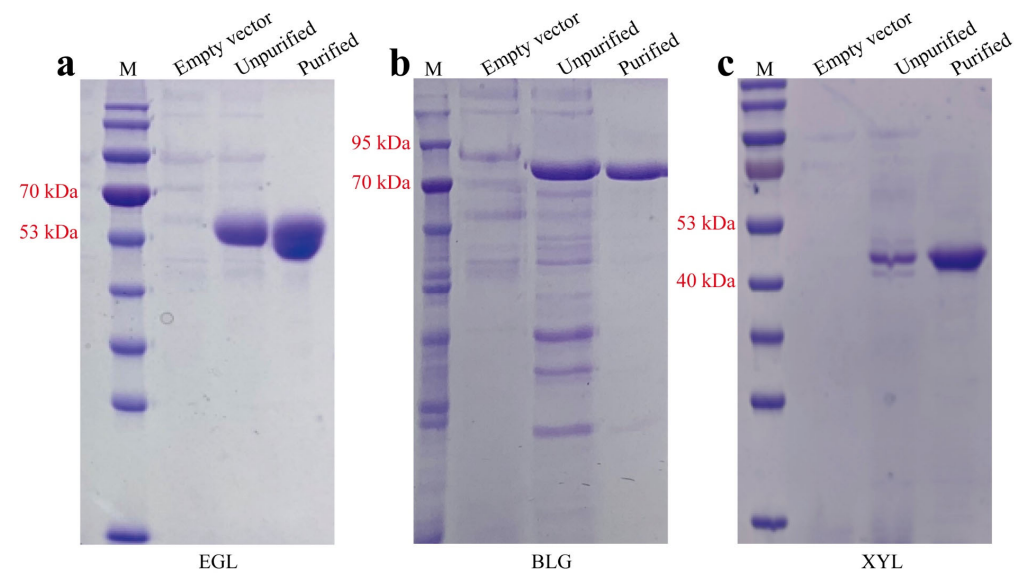


Figure 1. SDS-PAGE analysis of (a) EGL, (b) BGL, and (c) XYN, respectively. M: protein ladder; Empty vector: negative control; Unpurified: crude enzymes; Purified: purified proteins.

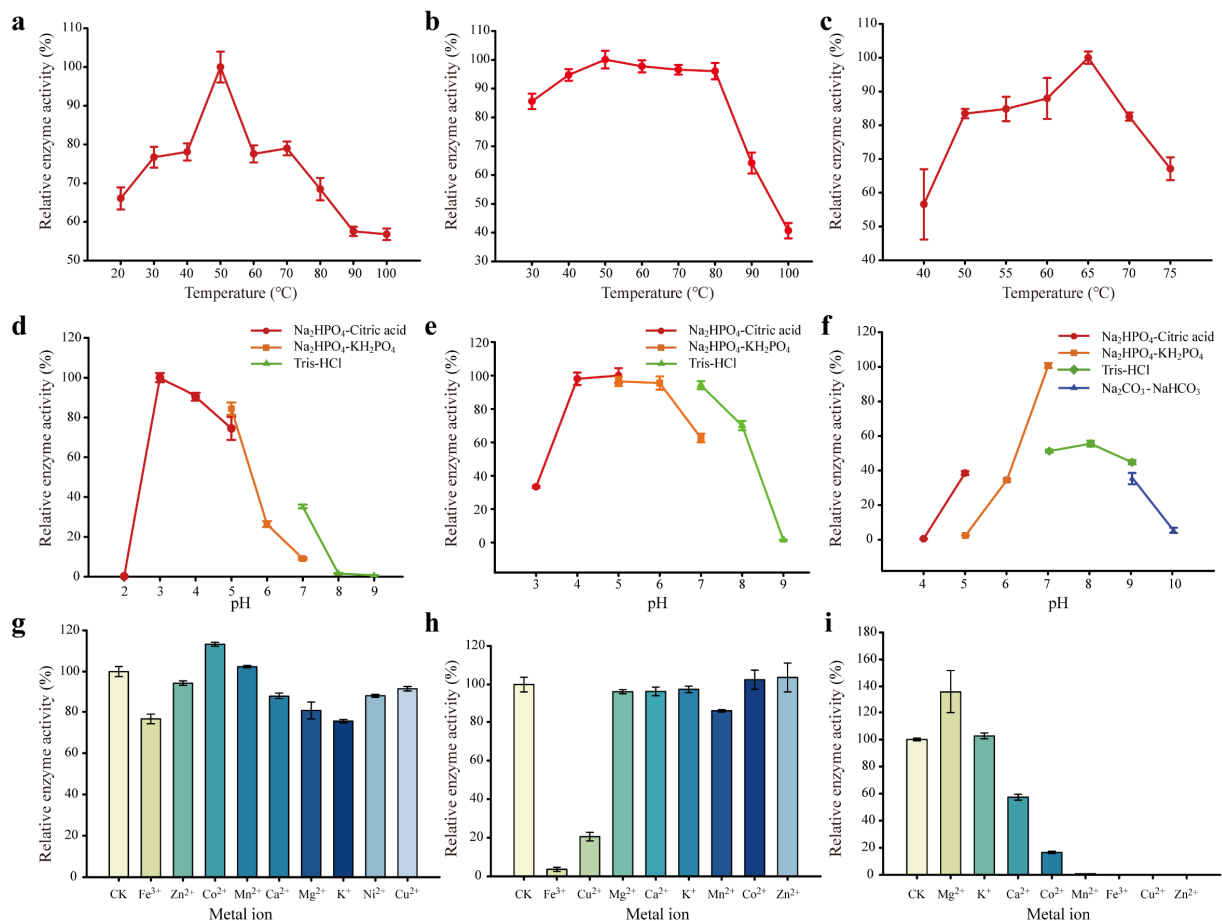


Figure 2. Enzymatic characteristics analysis of EGL, BGL, and XYN, respectively. (a–c) optimum temperature of EGL, BGL, and XYN; (d–f) optimum pH of EGL, BGL, and XYN; (g–i) the effects of different metal ions on the activities of EGL, BGL, and XYN. CK: no metal ions added as control group. The enzyme activity measured at different temperatures and pH conditions (a–f) was relative to the highest enzyme activity in these tests. Enzyme activity with the addition of different metal ions (g–i) was calculated relative to CK (without the addition of metal ions).

3.2. Kinetics Analysis of EGL, BGL, and XYN

Enzyme kinetics analysis is a scientific method used to examine the rate and reaction mechanism of enzyme-catalyzed reactions. This technique can be applied to study the catalytic efficiency and stability of enzymes under varying conditions, as well as to improve the production yield and specificity of enzymes. The maximum velocity of the reaction (V_{max}) and the Michaelis–Menten constant (K_m) are parameters that can be employed to characterize the affinity of an enzyme for its substrate and the reaction rate [38]. With CMC-Na as substrate, the highest V_{max} and K_m of EGL were $22.20 \mu\text{g}\cdot\text{mL}^{-1}\cdot\text{min}^{-1}$ and $1.03 \mu\text{g}\cdot\text{mL}^{-1}$ at pH 4.0, respectively (Figure S4). Similar to EGL, the catalytic rate of BGL exhibited a marked enhancement with increasing substrate concentration. The values of V_{max} and K_m of BGL with p-NPG as a substrate were $0.65 \mu\text{mol}\cdot\text{mL}^{-1}\cdot\text{min}^{-1}$ and $0.22 \mu\text{mol}\cdot\text{mL}^{-1}$, respectively (Figure S4), which further verified that BGL could utilize the soluble substrate effectively. As a hemicellulose-degrading enzyme, XYN demonstrated a higher V_{max} ($33.27 \mu\text{g}\cdot\text{mL}^{-1}\cdot\text{min}^{-1}$) and K_m ($1.28 \mu\text{g}\cdot\text{mL}^{-1}$) in comparison to EGL (Figure S4). The results indicated that EGL had a higher affinity for the substrate, minimizing the inhibitory effect of reducing oligosaccharides on the enzyme. Overall, these three enzymes exhibited relatively high reaction rates at relatively low substrate concentrations, indicating their strong affinity for the substrates.

3.3. Synergistic Degradation of Different Natural Substrates by EGL, BGL, and XYN

The efficiency of cellulose hydrolysis varies greatly among different lignocellulosic substrates, even when using the same cellulase preparation, due to variations in carbohydrate composition and physical properties that are dependent on the biomass type [39]. Therefore, it is necessary to optimize the mixing ratios of different enzymes in designing specific cellulase mixtures for the efficient degradation of lignocellulosic substrates [40]. In this study, different combinations of EGL, BGL, and XYN were employed for the synergistic degradation of four natural substrates, and the effect of different enzyme dosage ratios on the synergistic effect was also investigated. The combination of EGL and BGL showed a significantly better synergistic degradation of different natural substrates than EGL alone (Figure S5). It was speculated that the addition of BGL could promote the re-hydrolysis of the macromolecular products of lignocellulose hydrolyzed by EGL, thereby increasing the efficiency of lignocellulose hydrolysis. Additionally, the synergistic degradation effect of EGL and XYN on each natural substrate was significantly better than the treatment with XYN alone (Figure S6). Clearly, compared to the single-enzyme treatment, a mixture of cellulase and xylanase could result in higher hydrolysis of lignocellulosic substrates (Figure 3). Previous studies have shown that the combined use of xylanase and cellulase can increase the fiber width and decrease the fiber length of the substrate, as well as create small pores on the surface of the substrate, promoting the internal accessibility of cellulase [41,42]. It should be noted that excessive enzyme concentration might cause competition in the adsorption of substrates, leading to enzyme deactivation or poor substrate selectivity [43]. Therefore, the reasonable control of the dosage of cellulase and xylanase could maximize the degradation of lignocellulose. As shown in Figure 3, the increasing concentrations of EGL and BGL led to a gradual increase in the amount of reducing sugars produced by the synergistic hydrolysis of the three enzymes when using wheat straw, soybean straw, rice straw, and corn straw as substrates. Moreover, the combined action of the enzymes did not show a significant increase even at higher enzyme concentrations, once the ratios of EGL, BGL, and XYN reached a certain proportion (XYN:EGL:BGL = 10:7:7), particularly when using wheat straw and rice straw as substrates. This could be due to the competitive mechanism between the enzymes and substrates, which resulted in a balanced reaction rate at a certain level of total enzyme concentration, leading to a stable synergistic effect [43]. For soybean and corn stover, a good synergy effect could be achieved with less EGL and BGL added while keeping the same amount of xylanase. This might be due to the fact that xylanase changed the physical structure of the cellulose substrate, facilitating cellulase to enter cellulose more easily and penetrate the micro-fiber pores of cellulose, thus

accelerating the hydrolysis of the substrate. Overall, the combination of the three enzymes showed significantly better performance in hydrolyzing the substrate than the other two treatments, and the proportion of different enzyme additions also affected the degree of substrate degradation, but the underlying synergistic mechanism needs further exploration.

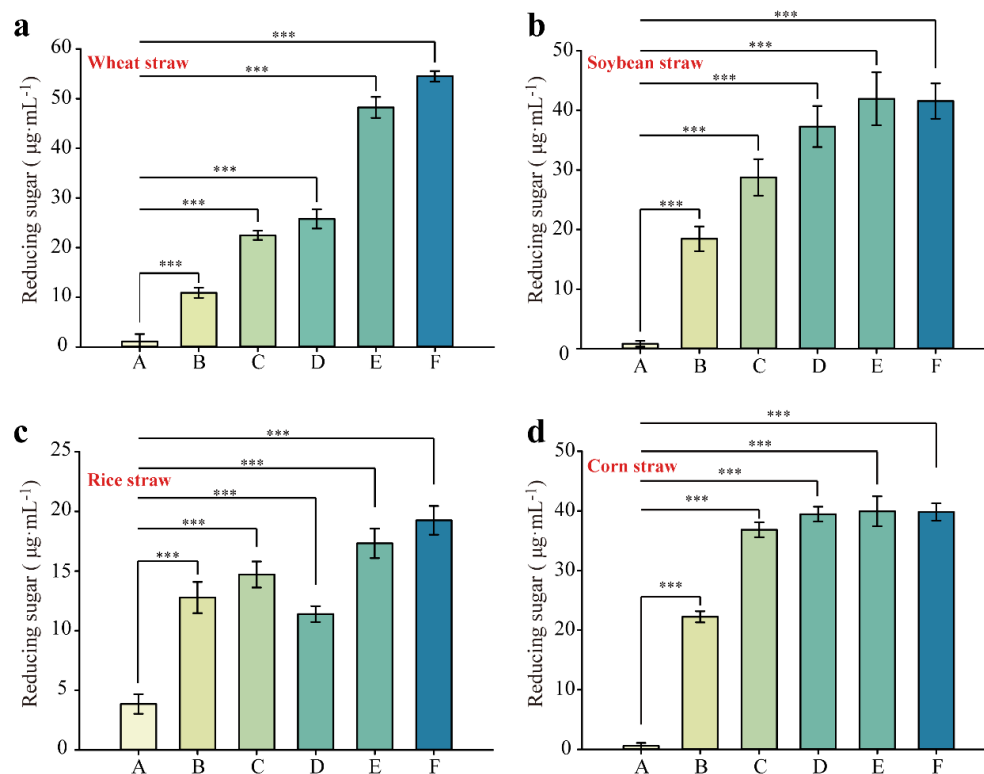


Figure 3. Synergistic degradation of different natural substrates by EGL, BGL, and XYN. (a) wheat straw; (b) soybean straw; (c) rice straw; (d) corn straw. Different letters on the x-axis represent different proportions of the three hydrolytic enzymes added. A: 0.1 M XYN; B: 0.1 M XYN + 0.01 M EGL + 0.01 M BGL; C: 0.1 M XYN + 0.03 M EGL + 0.03 M BGL; D: 0.1 M XYN + 0.05 M EGL + 0.05 M BGL; E: 0.1 M XYN + 0.07 M EGL + 0.07 M BGL; F: 0.1 M XYN + 0.09 M EGL + 0.09 M BGL. The volume of mixed enzyme solution added to all treatments was 10 µL. *** $p < 0.001$.

3.4. Evaluation of Functional Groups and Crystallinity of the Degraded Substrate

In the study of the hydrolysis products of lignocellulose, FTIR analysis is commonly performed to determine changes in the functional groups of substrates before and after hydrolysis [44]. After the hydrolysis of natural straw substrates by composite enzymes, the system exhibited characteristic absorption peaks including the O-H stretching vibration peak at 3400–3200 cm^{-1} , the saturated C-H peak at 3000–2800 cm^{-1} , the C=O peak at 1800–1600 cm^{-1} , and the C-O peak at 1300–1000 cm^{-1} [45]. Compared to CK, the FTIR spectra of natural straw substrates treated with three types of composite enzymes showed significant changes (Figure 4). In the case of wheat and soybean straw, the O-H and C-H peaks of the products after synergistic enzyme degradation exhibited a reduction in peak area, whereas in the case of rice straw, the areas of these peaks increased. This variability in degradation might be attributed to the structural diversity of the substrates. Enzymatic hydrolysis efficiency can be greatly impacted by the crystallinity of lignocellulosic materials, which refers to how ordered or packed the cellulose chains are within the material. To determine the crystallinity index, XRD is commonly used to analyze the scattering pattern and assess the relative contributions of crystalline fractions in the material [46]. In this study, XRD analysis revealed that the composite enzymes led to significant reductions in the crystallinity index of wheat straw (7.40%), soybean straw (2.37%), rice straw (20.60%), and corn straw (7.67%) in comparison to CK (Figure 5). The low crystallinity index indicates

the presence of a substantial amount of amorphous cellulose in the regenerated cellulose. Compared to highly crystalline cellulose, which has a strong interchain hydrogen-bonding network, amorphous cellulose has a larger surface area that can be easily accessed by cellulose enzymes [47]. As a result, the amorphous cellulose was easily hydrolyzed due to the combined action of these three enzymes, which could effectively target the crystalline regions of diverse natural substrates and modify their structure. This was especially apparent in rice straw, where the enzymes were able to significantly enhance the digestibility of the amorphous cellulose.

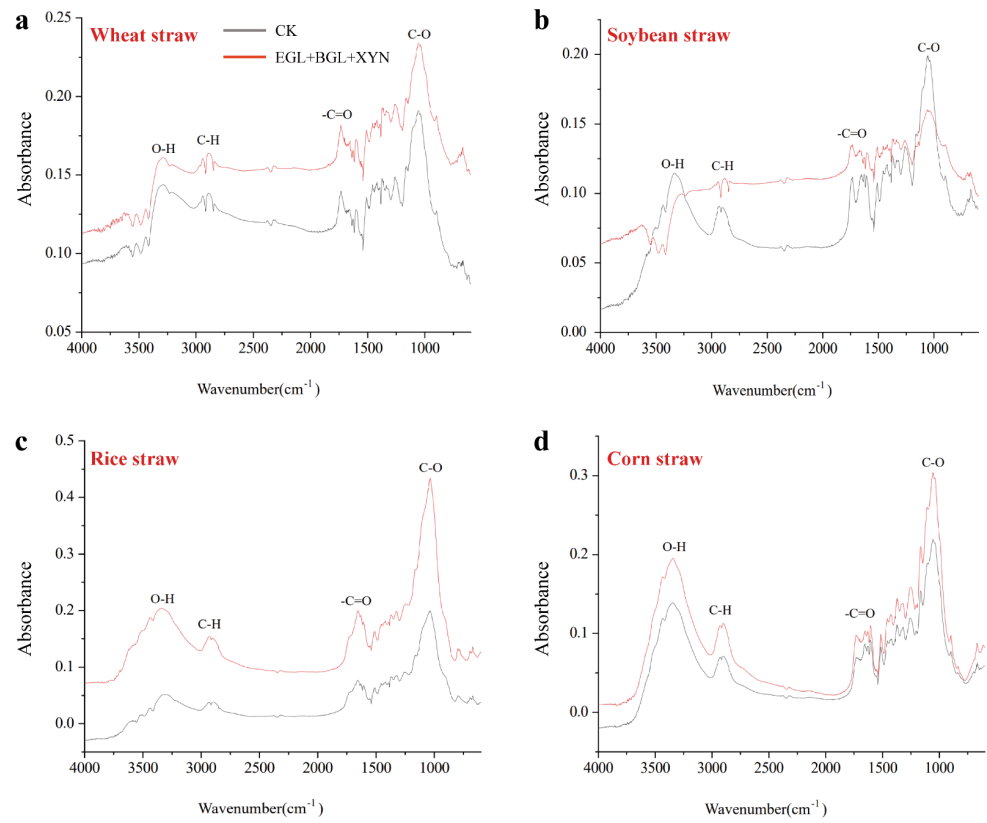


Figure 4. FTIR spectrum analysis of the substrate resulting from the degradation of various natural straws using a combination of enzymes. (a) wheat straw; (b) soybean straw; (c) rice straw; (d) corn straw. CK: natural straw; EGL + BGL + XYN: the substrates being treated by a combination of enzymes.

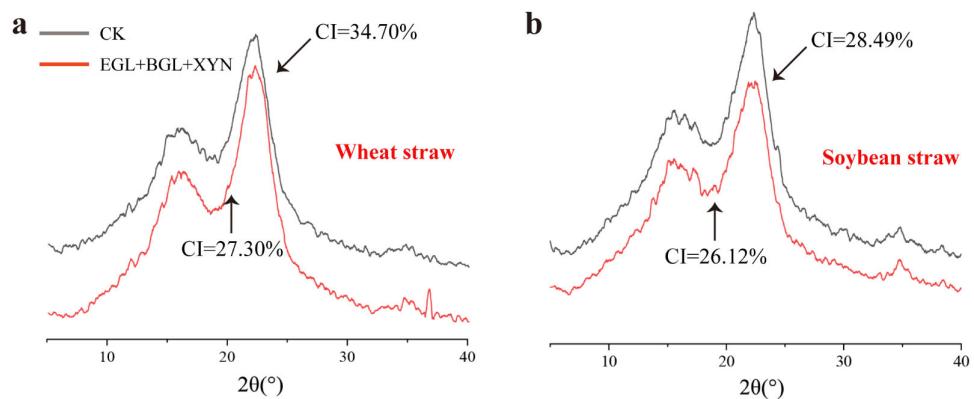


Figure 5. Cont.

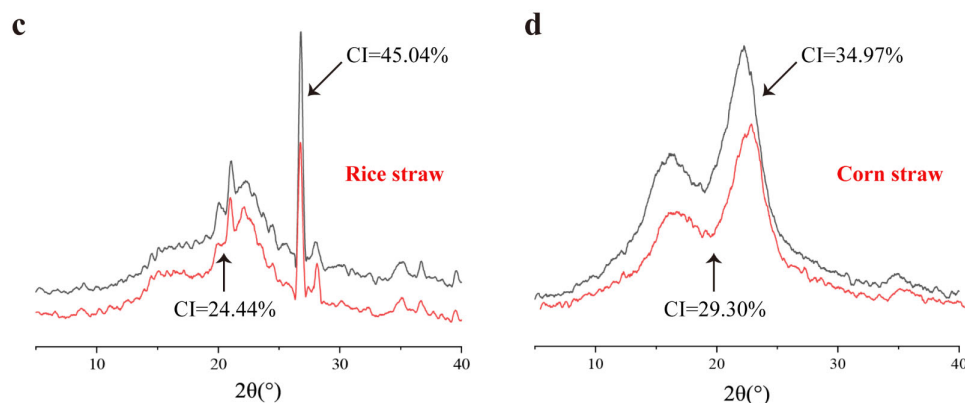


Figure 5. The crystallinity of the degraded substrate by XRD analysis. (a) wheat straw; (b) soybean straw; (c) rice straw; (d) corn straw. CK: natural straw; EGL + BGL + XYN: the substrates being treated by a combination of enzymes; CI: crystallinity index.

3.5. Scanning Electron Microscopy (SEM) Analysis

SEM is an important technique for demonstrating the extent of lignocellulose degradation by observing morphological changes before and after the hydrolysis process [48]. Untreated wheat straw had a high density and a clear and smooth structure. After hydrolysis by these three enzymes, the dense structure of wheat straw was disrupted, and surface degradation became more prominent, with the inner parenchyma beginning to be exposed (Figure 6a). The surface of untreated soybean straw exhibited a smooth, uniform, and highly ordered surface. In contrast, treatment with lignocellulases resulted in an uneven, rough, and rugged structure, giving the rice straw an overall unsmooth appearance (Figure 6b). Upon treatment, the outer parenchyma tissue of the rice straw disappeared partially, leaving the inner parenchyma tissue exposed. Additionally, the overall structure of the rice straw became more loosely packed, with an increase in the number of gaps and small fragments (Figure 6c). Interestingly, the morphology of corn stover changed dramatically after composite enzyme degradation. The stover was originally dense and intact in structure, but after hydrolysis, the surface became honeycombed and porous, indicating a more porous and less dense structure (Figure 6d). This porous structure provided greater access for cellulase enzymes to penetrate the cellulose fibers, thereby promoting the depolymerization and fragmentation of internal tissues [49].

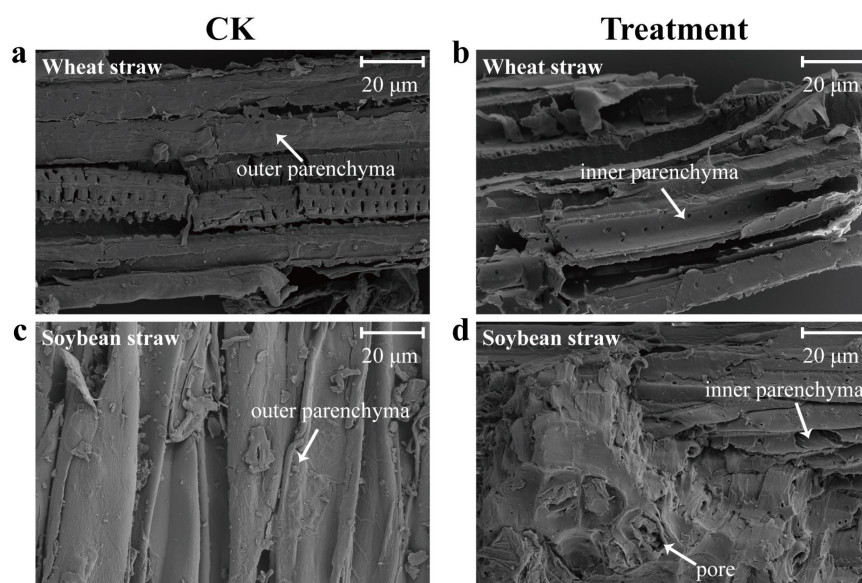


Figure 6. Cont.

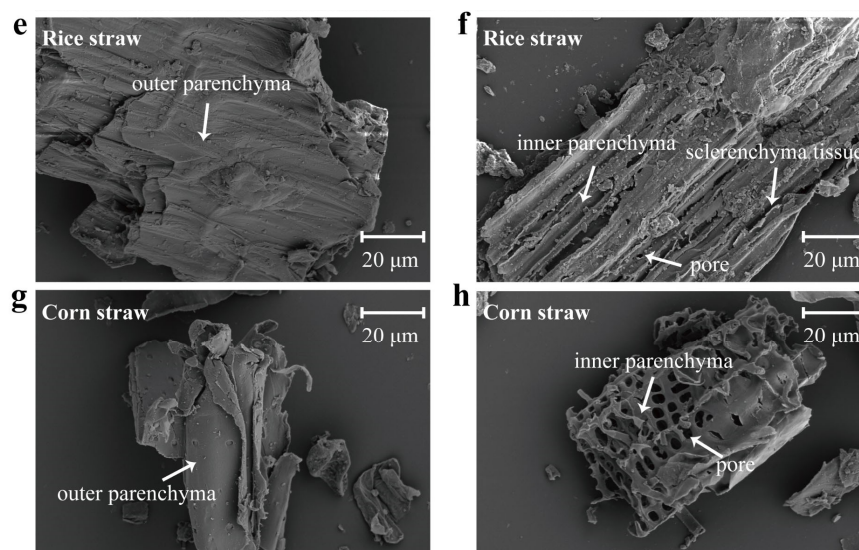


Figure 6. SEM analysis of raw and enzymatically hydrolyzed straw. (a,b) wheat straw; (c,d) soybean straw; (e,f) rice straw; (g,h) corn straw. Bar, 20 μm . CK: natural straw; Treatment: the substrates being treated by a combination of enzymes (EGL + BGL + XYN).

4. Conclusions

In this study, endoglucanase (EGL), β -glucosidase (BGL), and xylanase (XYN) from *Trichoderma guizhouense* NJAU4742 were characterized. These three enzymes exhibited a wide range of temperature and pH adaptability and showed varying preferences for different metal ions. Meanwhile, four types of natural agricultural straws were utilized as substrates, and the ideal combination ratio of the three enzymes for synergistic degradation was determined. Additionally, the results demonstrated that the synergistic action of these three enzymes could result in the depolymerization and breaking of the substrate structure, shifts and changes in the absorption peaks of functional groups, and a decrease in crystallinity. This study will provide a reliable understanding of the synergistic mechanism between lignocellulase systems, contributing theoretical support to improving the efficiency of agricultural solid waste degradation.

Supplementary Materials: The following supporting information can be downloaded at: <https://www.mdpi.com/article/10.3390/fermentation10050230/s1>, Figure S1: The phylogenetic trees of EGL by performing multiple sequence alignments using MEGAX software; Figure S2: The phylogenetic trees of BGL by performing multiple sequence alignments using MEGAX software; Figure S3: The phylogenetic trees of XYN by performing multiple sequence alignments using MEGAX software; Figure S4: Kinetic analysis of EGL (a), BLG (b), and XYN (c), respectively; Figure S5: Synergistic degradation of different natural substrates by EGL and BGL; Figure S6: Synergistic degradation of different natural substrates by EGL and XYN.

Author Contributions: T.L.: methodology, software, supervision, writing—original draft, writing—review, and editing. R.P.: methodology and formal analysis. J.W.: investigation and software. Y.Z.: investigation and validation. D.L.: writing—review, editing, supervision, and data curation. All authors have read and agreed to the published version of the manuscript.

Funding: This research was funded by National Natural Science Foundation of China, grant number 32172680 and 32302679; Natural Science Foundation of Jiangsu Province, grant number BK20230991; and the National Postdoctoral Research Fellowship Program, grant number GZC20231126.

Data Availability Statement: Source data that support the findings of this study are available from the corresponding author on reasonable request.

Conflicts of Interest: The authors declare that they have no known competing financial interests or personal relationships that could have appeared to influence the work reported in this paper.

Abbreviations

Abbreviation	Definition
EGL	Endoglucanase
BGL	β -glucosidase
XYN	Xylanase
CK	Control
SEM	Scanning electron microscopy
FTIR	Fourier transform infrared spectroscopy
XRD	X-ray diffraction
CI	Crystallinity index

References

1. Rezai, A.; Van Der Ploeg, F. Abandoning fossil fuel: How fast and how much. *Manch. Sch.* **2017**, *85*, e16–e44. [[CrossRef](#)]
2. Lin, B.; Xu, B. How does fossil energy abundance affect China's economic growth and CO₂ emissions? *Sci. Total Environ.* **2020**, *719*, 137503. [[CrossRef](#)] [[PubMed](#)]
3. Alzoubi, A. Renewable Green hydrogen energy impact on sustainability performance. *Int. J. Comput. Inf. Manuf.* **2021**, *1*, 1. [[CrossRef](#)]
4. Malherbe, S.; Cloete, T.E. Lignocellulose biodegradation: Fundamentals and applications. *Rev. Environ. Sci. Biotechnol.* **2002**, *1*, 105–114. [[CrossRef](#)]
5. Jurgens, G.; Survase, S.; Berezina, O.; Sklavounos, E.; Linnekoski, J.; Kurkijärvi, A.; Väkevä, M.; van Heiningen, A.; Granström, T. Butanol production from lignocellulosics. *Biotechnol. Lett.* **2012**, *34*, 1415–1434. [[CrossRef](#)] [[PubMed](#)]
6. Margeot, A.; Hahn-Hagerdal, B.; Edlund, M.; Slade, R.; Monot, F. New improvements for lignocellulosic ethanol. *Curr. Opin. Biotechnol.* **2009**, *20*, 372–380. [[CrossRef](#)]
7. Hamawand, I.; Seneweera, S.; Kumarasinghe, P.; Bundschuh, J. Nanoparticle technology for separation of cellulose, hemicellulose and lignin nanoparticles from lignocellulose biomass: A short review. *Nano Struct. Nano Objects* **2020**, *24*, 100601. [[CrossRef](#)]
8. Sharma, H.K.; Xu, C.; Qin, W. Biological pretreatment of lignocellulosic biomass for biofuels and bioproducts: An overview. *Waste Biomass Valorization* **2019**, *10*, 235–251. [[CrossRef](#)]
9. Zupančič, G.D.; Grilc, V. Anaerobic treatment and biogas production from organic waste. In *Management of Organic Waste*; Institute for Environmental Protection and Sensor: Ljubljana, Slovenia, 2012; p. 2.
10. Zhang, Y.P. Reviving the carbohydrate economy via multi-product lignocellulose biorefineries. *J. Ind. Microbiol. Biotechnol.* **2008**, *35*, 367–375. [[CrossRef](#)]
11. Juturu, V.; Wu, J.C. Microbial cellulases: Engineering, production and applications. *Renew. Sustain. Energy Rev.* **2014**, *33*, 188–203. [[CrossRef](#)]
12. Himmel, M.E.; Ding, S.-Y.; Johnson, D.K.; Adney, W.S.; Nimlos, M.R.; Brady, J.W.; Foust, T.D. Biomass recalcitrance: Engineering plants and enzymes for biofuels production. *Science* **2007**, *315*, 804–807. [[CrossRef](#)] [[PubMed](#)]
13. Chundawat, S.P.; Beckham, G.T.; Himmel, M.E.; Dale, B.E. Deconstruction of lignocellulosic biomass to fuels and chemicals. *Annu. Rev. Chem. Biomol. Eng.* **2011**, *2*, 121–145. [[CrossRef](#)] [[PubMed](#)]
14. Zaldivar, J.; Nielsen, J.; Olsson, L. Fuel ethanol production from lignocellulose: A challenge for metabolic engineering and process integration. *Appl. Microbiol. Biotechnol.* **2001**, *56*, 17–34. [[CrossRef](#)] [[PubMed](#)]
15. Kumar, A.; Chandra, R. Ligninolytic enzymes and its mechanisms for degradation of lignocellulosic waste in environment. *Heliyon* **2020**, *6*, e03170. [[CrossRef](#)] [[PubMed](#)]
16. Kim, I.J.; Lee, H.J.; Choi, I.-G.; Kim, K.H. Synergistic proteins for the enhanced enzymatic hydrolysis of cellulose by cellulase. *Appl. Microbiol. Biotechnol.* **2014**, *98*, 8469–8480. [[CrossRef](#)] [[PubMed](#)]
17. Wang, M.; Liu, K.; Dai, L.; Zhang, J.; Fang, X. The structural and biochemical basis for cellulose biodegradation. *J. Chem. Technol. Biotechnol.* **2013**, *88*, 491–500. [[CrossRef](#)]
18. Rani, V.; Mohanram, S.; Tiwari, R.; Nain, L.; Arora, A. Beta-glucosidase: Key enzyme in determining efficiency of cellulase and biomass hydrolysis. *J. Bioprocess. Biotech.* **2014**, *5*, 197.
19. Motta, F.; Andrade, C.; Santana, M. A review of xylanase production by the fermentation of xylan: Classification, characterization and applications. *Sustain. Degrad. Lignocellul. Biomass Tech. Appl. Commer.* **2013**, *1*, 251–276.
20. Bischof, R.H.; Ramoni, J.; Seiboth, B. Cellulases and beyond: The first 70 years of the enzyme producer *Trichoderma reesei*. *Microb. Cell Factories* **2016**, *15*, 106. [[CrossRef](#)]
21. Häkkinen, M.; Arvas, M.; Oja, M.; Aro, N.; Penttilä, M.; Saloheimo, M.; Pakula, T.M. Re-annotation of the CAZy genes of *Trichoderma reesei* and transcription in the presence of lignocellulosic substrates. *Microb. Cell Factories* **2012**, *11*, 134. [[CrossRef](#)]
22. Schuster, A.; Schmoll, M. Biology and biotechnology of *Trichoderma*. *Appl. Microbiol. Biotechnol.* **2010**, *87*, 787–799. [[CrossRef](#)] [[PubMed](#)]

23. Qualhato, T.F.; Lopes, F.A.C.; Steindorff, A.S.; Brandao, R.S.; Jesuino, R.S.A.; Ulhoa, C.J. Mycoparasitism studies of *Trichoderma* species against three phytopathogenic fungi: Evaluation of antagonism and hydrolytic enzyme production. *Biotechnol. Lett.* **2013**, *35*, 1461–1468. [[CrossRef](#)] [[PubMed](#)]
24. Xia, Y.; Wang, J.; Guo, C.; Xu, H.; Wang, W.; Yang, M.; Shen, Q.; Zhang, R.; Miao, Y. Exploring the multi-level regulation of lignocellulases in the filamentous fungus *Trichoderma guizhouense* NJAU4742 from an omics perspective. *Microb. Cell Factories* **2022**, *21*, 144. [[CrossRef](#)] [[PubMed](#)]
25. Li, T.; Kong, Z.; Zhang, X.; Wang, X.; Chai, L.; Liu, D.; Shen, Q. Deciphering the effect of exogenous lignocellulases addition on the composting efficiency and microbial communities. *Bioresour. Technol.* **2022**, *361*, 127751. [[CrossRef](#)] [[PubMed](#)]
26. Liu, D.; Li, J.; Zhao, S.; Zhang, R.; Wang, M.; Miao, Y.; Shen, Y.; Shen, Q. Secretome diversity and quantitative analysis of cellulolytic *Aspergillus fumigatus* Z5 in the presence of different carbon sources. *Biotechnol. Biofuels* **2013**, *6*, 149. [[CrossRef](#)] [[PubMed](#)]
27. Wu, Q.; Fan, G.; Yu, T.; Sun, B.; Tang, H.; Teng, C.; Yang, R.; Li, X. Biochemical characteristics of the mutant xylanase T-XynC (122) C (166) and production of xylooligosaccharides from corncobs. *Ind. Crop. Prod.* **2019**, *142*, 111848. [[CrossRef](#)]
28. Bansal, P.; Hall, M.; Realf, M.J.; Lee, J.H.; Bommarius, A.S. Modeling cellulase kinetics on lignocellulosic substrates. *Biotechnol. Adv.* **2009**, *27*, 833–848. [[CrossRef](#)] [[PubMed](#)]
29. Hu, R.; Lin, L.; Liu, T.; Ouyang, P.; He, B.; Liu, S. Reducing sugar content in hemicellulose hydrolysate by DNS method: A revisit. *J. Biobased Mater. Bioenergy* **2008**, *2*, 156–161. [[CrossRef](#)]
30. Basotra, N.; Kaur, B.; Di Falco, M.; Tsang, A.; Chadha, B.S. Mycothermus thermophilus (Syn. *Scytalidium thermophilum*): Repertoire of a diverse array of efficient cellulases and hemicellulases in the secretome revealed. *Bioresour. Technol.* **2016**, *222*, 413–421. [[CrossRef](#)]
31. Kim, S.B.; Lee, S.J.; Lee, J.H.; Jung, Y.R.; Thapa, L.P.; Kim, J.S.; Um, Y.; Park, C.; Kim, S.W. Pretreatment of rice straw with combined process using dilute sulfuric acid and aqueous ammonia. *Biotechnol. Biofuels* **2013**, *6*, 109. [[CrossRef](#)]
32. Segal, L.; Creely, J.J.; Martin Jr, A.; Conrad, C. An empirical method for estimating the degree of crystallinity of native cellulose using the X-ray diffractometer. *Text. Res. J.* **1959**, *29*, 786–794. [[CrossRef](#)]
33. McDonald, J.E.; Houghton, J.N.; Rooks, D.J.; Allison, H.E.; McCarthy, A.J. The microbial ecology of anaerobic cellulose degradation in municipal waste landfill sites: Evidence of a role for fibrobacters. *Environ. Microbiol.* **2012**, *14*, 1077–1087. [[CrossRef](#)] [[PubMed](#)]
34. de Cassia Pereira, J.; Giese, E.C.; de Souza Moretti, M.M.; dos Santos Gomes, A.C.; Perrone, O.M.; Boscolo, M.; da Silva, R.; Gomes, E.; Martins, D.A.B. Effect of metal ions, chemical agents and organic compounds on lignocellulolytic enzymes activities. *Enzym. Inhib. Act.* **2017**, *29*, 139–164.
35. Zhou, Y.; Yang, J.; Luo, C.; Yang, B.; Liu, C.; Xu, B. Effect of metal ions and surfactants on the enzymatic hydrolysis of pretreated lignocellulose. *BioResources* **2019**, *14*, 1653–1667. [[CrossRef](#)]
36. Corrêa, A.P.F.; Daroit, D.J.; Brandelli, A. Characterization of a keratinase produced by *Bacillus* sp. P7 isolated from an Amazonian environment. *Int. Biodeterior. Biodegrad.* **2010**, *64*, 1–6. [[CrossRef](#)]
37. Andreini, C.; Bertini, I.; Cavallaro, G.; Holliday, G.L.; Thornton, J.M. Metal ions in biological catalysis: From enzyme databases to general principles. *J. Biol. Inorg. Chem.* **2008**, *13*, 1205–1218. [[CrossRef](#)] [[PubMed](#)]
38. Beltrame, P.L.; Carniti, P.; Fochoer, B.; Marzetti, A.; Sarto, V. Enzymatic hydrolysis of cellulosic materials: A kinetic study. *Biotechnol. Bioeng.* **1984**, *26*, 1233–1238. [[CrossRef](#)] [[PubMed](#)]
39. Banerjee, G.; Car, S.; Scott-Craig, J.S.; Borrusch, M.S.; Walton, J.D. Rapid optimization of enzyme mixtures for deconstruction of diverse pretreatment/biomass feedstock combinations. *Biotechnol. Biofuels* **2010**, *3*, 22. [[CrossRef](#)] [[PubMed](#)]
40. Berlin, A.; Maximenko, V.; Gilkes, N.; Saddler, J. Optimization of enzyme complexes for lignocellulose hydrolysis. *Biotechnol. Bioeng.* **2007**, *97*, 287–296. [[CrossRef](#)]
41. Arantes, V.; Gourlay, K.; Saddler, J.N. The enzymatic hydrolysis of pretreated pulp fibers predominantly involves “peeling/erosion” modes of action. *Biotechnol. Biofuels* **2014**, *7*, 87. [[CrossRef](#)]
42. Hu, J.; Gourlay, K.; Arantes, V.; Van Dyk, J.; Pribowo, A.; Saddler, J.N. The accessible cellulose surface influences cellulase synergism during the hydrolysis of lignocellulosic substrates. *ChemSusChem* **2015**, *8*, 901–907. [[CrossRef](#)] [[PubMed](#)]
43. Song, H.-T.; Gao, Y.; Yang, Y.-M.; Xiao, W.-J.; Liu, S.-H.; Xia, W.-C.; Liu, Z.-L.; Yi, L.; Jiang, Z.-B. Synergistic effect of cellulase and xylanase during hydrolysis of natural lignocellulosic substrates. *Bioresour. Technol.* **2016**, *219*, 710–715. [[CrossRef](#)] [[PubMed](#)]
44. Spiridon, I.; Teaca, C.A.; Bodirlau, R. Structural changes evidenced by FTIR spectroscopy in cellulosic materials after pre-treatment with ionic liquid and enzymatic hydrolysis. *BioResources* **2011**, *6*, 400–413. [[CrossRef](#)]
45. Yang, X.; Zhao, Y.; Li, R.; Wu, Y.; Yang, M. A modified kinetic analysis method of cellulose pyrolysis based on TG–FTIR technique. *Thermochim. Acta* **2018**, *665*, 20–27. [[CrossRef](#)]
46. Bian, J.; Peng, F.; Peng, X.-P.; Xiao, X.; Peng, P.; Xu, F.; Sun, R.-C. Effect of [Emim] Ac pretreatment on the structure and enzymatic hydrolysis of sugarcane bagasse cellulose. *Carbohydr. Polym.* **2014**, *100*, 211–217. [[CrossRef](#)] [[PubMed](#)]
47. Yoon, L.W.; Ang, T.N.; Ngoh, G.C.; Chua, A.S.M. Regression analysis on ionic liquid pretreatment of sugarcane bagasse and assessment of structural changes. *Biomass Bioenergy* **2012**, *36*, 160–169. [[CrossRef](#)]

48. Dar, M.A.; Shaikh, A.A.; Pawar, K.D.; Pandit, R.S. Exploring the gut of *Helicoverpa armigera* for cellulose degrading bacteria and evaluation of a potential strain for lignocellulosic biomass deconstruction. *Process Biochem.* **2018**, *73*, 142–153. [[CrossRef](#)]
49. Arantes, V.; Saddler, J.N. Cellulose accessibility limits the effectiveness of minimum cellulase loading on the efficient hydrolysis of pretreated lignocellulosic substrates. *Biotechnol. Biofuels* **2011**, *4*, 3. [[CrossRef](#)]

Disclaimer/Publisher’s Note: The statements, opinions and data contained in all publications are solely those of the individual author(s) and contributor(s) and not of MDPI and/or the editor(s). MDPI and/or the editor(s) disclaim responsibility for any injury to people or property resulting from any ideas, methods, instructions or products referred to in the content.